COBEM 2021 26th International Congress of Mechanical Engineering
November 22-26, 2021, Virtual Congress, Brazil

COB-2021-1526
A COMPARATIVE STUDY OF RANS TURBULENCE CLOSURE MODELS AND INFLUENCE OF WIND DIRECTION IN A BUILDING ARRAY

Gabriel Gusmão Almeida
Fernanda Capucho Cezana
Federal Institute of Science and Technology of Espírito Santo
gabrielgusmaoalmeida@hotmail.com
fecezana@ifes.edu.br

Abstract. *In the present paper we have tested four different turbulence closure models based on Reynolds Averaged Navier- Stokes (RANS) methodology. The characteristics around a group of obstacles are investigated numerically focusing on the influence of wind direction in a building array. The mathematical modeling is based on the solution of the conservation equations (mass and momentum). Numerical simulations were performed over an idealized urban canopy with twenty-four unequally spaced buildings with rectangular cross sections and constant height with a commercial software ANSYS-FLUENT 16.0, that use a finite volume method. Wind direction influence was analyzed and discussed. It was found that the flow pattern is affected by the wind direction, with the formation of recirculation zones and low-velocity regions.*

Keywords: *Turbulence modelling, Group of obstacles, Urban Area, Wind direction*

1. INTRODUCTION

The intense urbanization promotes the construction of many buildings in urban areas, which affects the local wind flow and contributes to the pollutant accumulation, resulting in air quality problems. There is a vast literature on modelling and numerical simulation of the flow and pollutant dispersion in urban areas (Carpentieri and Robins, 2015; Chen *et al.*, 2017; Goulart *et al.*, 2019). In particular, numerous numerical investigations have focused on modelling using RANS (Reynolds Averaged Navier-Stokes) (Ramponi *et al.*, 2015, Buccolieri *et al.*, 2015, Ricci *et al.*, 2020).

As pointed out by An and Fung (2018), Hong Kong's urbanization brought an increase in the number of skyscrapers present at the city, creating urban canopies that together with the heavy traffic and the entanglement of many streets, it enhances the local pollutant concentration.

Ramponi *et al.* (2015) presented a literature review addressing ventilation in urban environments and ventilation efficiency in removing air pollutants. The authors highlighted the use of RANS for modelling turbulence in a series of studies. They also highlighted that LES has a high computational cost and that RANS, despite its limitations, is a good alternative, presenting a very good performance even for more complex urban configurations.

Buccolieri *et al.* (2015) used RANS to investigate the conditions of pollutant dispersion in dense building arrays with packing densities like those of typical European cities. A vast literature review was carried out regarding the use of RANS to calculate the flow and dispersion of pollutants in urban areas. The authors showed that this methodology is still widely used to investigate the main characteristics of the mechanisms of ventilation and dispersion of pollutants in urban canyons and urban canopies.

Therefore, the main aim of this work consists of investigating the performance of four Reynolds Averaged Navier-Stokes (RANS) turbulence closure models and the influence of wind direction in a building array.

2. METHODOLOGY

In the present paper the air flow in an idealized urban environment was investigated using numerical simulation. Figure 1 shows the computational domain, that was defined according to the wind tunnel experiment developed by Carpentieri and Robins (2015), with all buildings of constant height, $H_b = 102$ mm. The buildings blocks occupy an area of 230×350 mm² each and the Reynolds number based on the building height in the experimental conditions was $Re \approx 1.7 \cdot 10^4$. The reference wind measured at 1 m height was $U_{REF} = 2.5$ m s^{-1}. The origin of the coordinate system is in the center of the model, i.e., at the ground of the major intersection. More details of wind tunnel experiments are described in Carpentieri and Robins (2015).

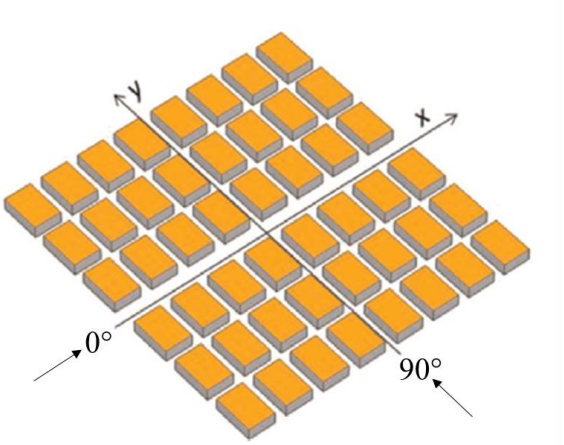

Figure 1. 3D representation of the model (Carpentieri and Robins (2015)).

2.1 Governing equations and Numerical method

The governing equations for the atmospheric flow in neutral conditions, considering an incompressible flow and a steady-state regime based on the Reynolds Averaged Navier Stokes approach are presented below.

$$\frac{\partial \overline{u_j}}{\partial x_j} = 0, \tag{1}$$

$$\rho \frac{\partial \overline{u_i}\overline{u_j}}{\partial x_j} = -\frac{\partial \overline{p}}{\partial x_i} + g\delta_{i3} + \mu \frac{\partial^2 \overline{u_i}}{\partial x_j \partial x_j} + \frac{\partial \tau_{ij}}{\partial x_j}. \tag{2}$$

Where $\overline{u_i}$ is the mean velocity component in the i direction, ρ is the fluid density, μ is the absolute viscosity of the fluid, $\overline{p}$ is the mean pressure and g is the gravitational acceleration. In general, the flow in the atmosphere is turbulent, particularly in an urban area it turns out to be extremely complex, tridimensional and irregular.

To close the system of equations, knowing that the Reynolds decomposition creates an unknown term τ_{ij}, we should model this term, which can be done in many ways. In the two-equation turbulence closure models, τ_{ij} is modeled as follows:

$$\tau_{ij} = -\rho \overline{u_i' u_j'} = \mu_t (2S_{ij}) - \frac{2}{3}\rho k \delta_{ij}, \tag{3}$$

$$k = \frac{\overline{u_i' u_i'}}{2}. \tag{4}$$

Where,

$$S_{ij} = \frac{1}{2}\left(\frac{\partial \overline{u_i}}{\partial x_j} + \frac{\partial \overline{u_j}}{\partial x_i}\right), \tag{5}$$

is the mean strain rate tensor, μ_t is the turbulent viscosity, k is the turbulent kinetic energy, ε is the turbulent kinetic energy dissipation rate and ω is the turbulent kinetic energy dissipation frequency. With that, μ_t is defined in terms of k and ε in the Standard $k-\varepsilon$ (Launder and Spalding, 1972) and RSM (Reynolds Stress Model) Linear Pressure-Strain (Gibson and Launder, 1978; Fu et al, 1987; Launder, 1989) models, and in terms of k and ω in the $k-\omega$ SST (Menter, 1994) and RSM Stress-Omega (Wilcox, 1998) models.

The equations are numerically solved in steady-state regime, using the finite volume method of *Ansys Fluent* 16.0 computational code. Aiming to show that our numerical solution does not depend on the used mesh, a mesh sensibility test was taken, but it is not shown. The same simulation conditions are tested in four levels of mesh discretization: 1, 2, 3 and 4 million nodes, with the Standard $k-\varepsilon$ model and the Navier-Stokes equation was discretized using a second-order scheme in space. It was possible to verify that the solutions of these meshes converged to finest one, with 4 million nodes.

However, it was seen that the solution given by the 3 million one is quite close to the 4 million one, therefore, the 3 million one was chosen for being the most computationally advantageous. A four-level hexahedral mesh (3 million cells) with $13 \times 29 \times 42$ cells per building blocks ($H_b \times 2{,}3H_b \times 3{,}5H_b$ dimensions of the building blocks, , approximately) in the near wall region (see Figure 2) were used.

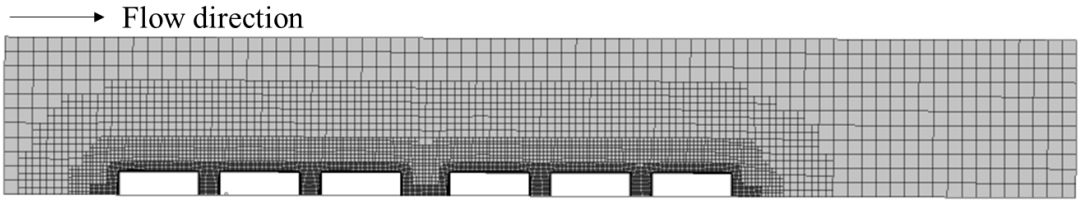

(a)

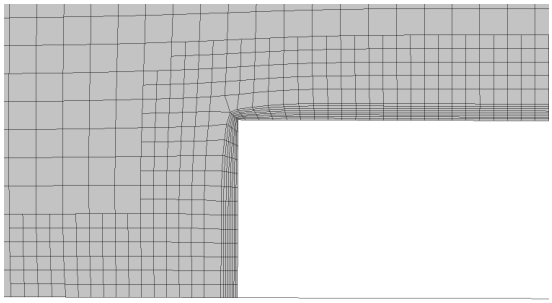

(b)

Figure 2: Hexahedral mesh (a) $13 \times 29 \times 42$ cells per building block, 3 million cells; (b) zoom showing the mesh in the near wall region.

2.2 Boundary conditions

Table 1 shows boundary conditions used in this study, where $u_* = 0{,}06U_{REF}$, $U_{REF} = 2{,}5\ \mathrm{m}s^{-1}$ is the free stream velocity, $\kappa = 0{,}4187$ is the Von Karman constant, $z_o = 0{,}015H_b$ and $C_\mu = 0{,}09$.

Table 1. Boundary conditions

Inlet	Velocity profile U was taken as wind tunnel measurements (Carpentieri and Robins, 2015), $k = \frac{u_*^2}{\sqrt{C_\mu}}, \varepsilon = \frac{u_*^3}{\kappa z}, \omega = \frac{\sqrt{k}}{\sqrt[4]{C_\mu}\kappa z}$
Outlet	Zero static pressure (outflow condition)
Laterals and top	Symmetry
Buildings walls and bottom	No-slip

3. RESULTS AND DISCUSSION

Given that the geometry, governing equations and boundary conditions to be used are determined, the different turbulence closure models were then tested and the one that better described the flow was used in the analysis of the wind direction influence.

3.1 RANS results compared with wind tunnel and a comparison of different turbulence closure models

Vertical profiles of the mean horizontal velocity, V, at two positions (see Figure 3) obtained using four different turbulence closure models, Standard k - ε, SST k - ω, the Reynolds Stress Linear Pressure-Strain (RSM k-ε) and the Stress-Omega Models (RSM k-ω), are shown in Figure 4. The results are in satisfactory agreement with wind tunnel measurements (Carpentieri and Robins, 2015). Note that all models have a similar behavior. However, the results of RSM

k-ω model agree better than the other ones in the canopy. The RSM k-ω model was proposed by Wilcox (1998), and it is based on $k - \omega$ equations. According to the author, the advantage of using the k and ω equations is that it allows a more appropriate boundary condition for walls, including flows with boundary-layer separation and with low Reynolds numbers. Above the canopy, numerical results and wind tunnel clearly to disagree. Table 2 displays all model's accuracy through a mean percentage relative error, which was calculated using experimental points within $z/H_b \leq 1$, since only the data points inside the canopy are useful to this study, then the errors obtained for each position were averaged to better comparison between models.

Nonetheless, the focus of the study is to understand the flow's behavior inside and just above the urban canopy, therefore, as shown in Table 2, the RSM k-ω is the best model in this region, although the other models represented better the flow in the free stream region.

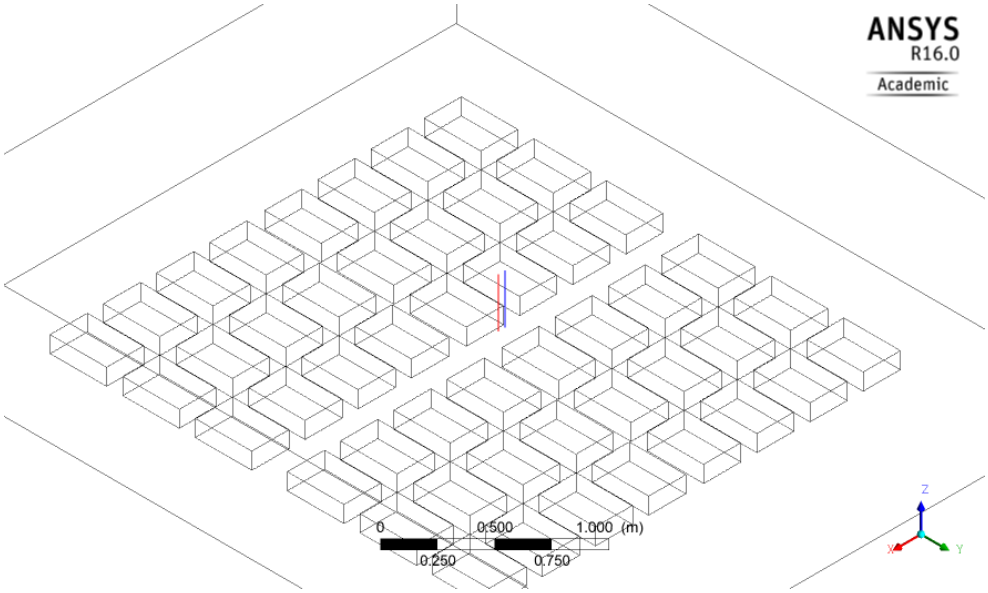

Figure 3. Location of the lines from which the vertical profile of the mean horizontal velocity was obtained.

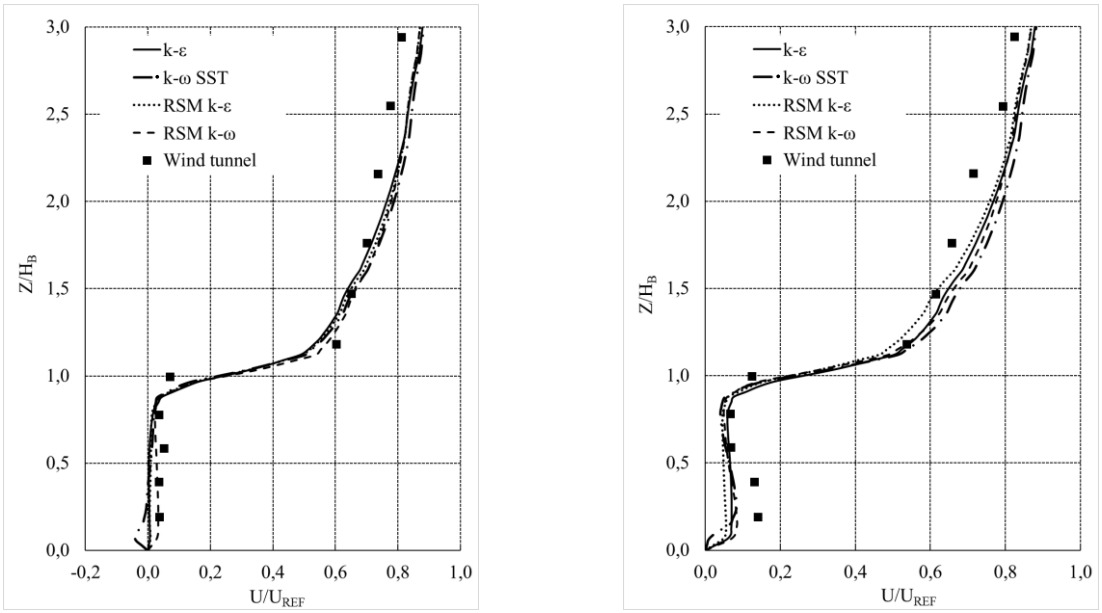

(a) (b)

Figure 4. Vertical profile of the mean horizontal velocity at $y/H_b = -0{,}88$, wind direction 90° at (a) $x/H_b = -2{,}30$ and (b)$x/H_b = -2{,}70$, for four different turbulence closure models.

Table 2. Mean percentage relative error of the models for the vertical profile of the mean horizontal velocity.

Position at $y/H_b = -0{,}88$	Standard $k-\varepsilon$	RSM Linear Pressure-Strain	$k-\omega$ SST	RSM Stress-Omega
$x/H_b = -2{,}30$ (Shown in Figure 4a)	-80%	-78%	-88%	-25%
$x/H_b = -2{,}70$ (Shown in Figure 4b)	-12%	-31%	-23%	-20%
Average	**-46%**	**-54%**	**-56%**	**-22%**

3.2 Influence of wind direction

Figure 5 presents a contour plot of mean horizontal velocity at two different heights from the ground and for two different wind directions, 0° and 90°. Note that the velocity varies with height and to show the details, different colourmaps have been used.

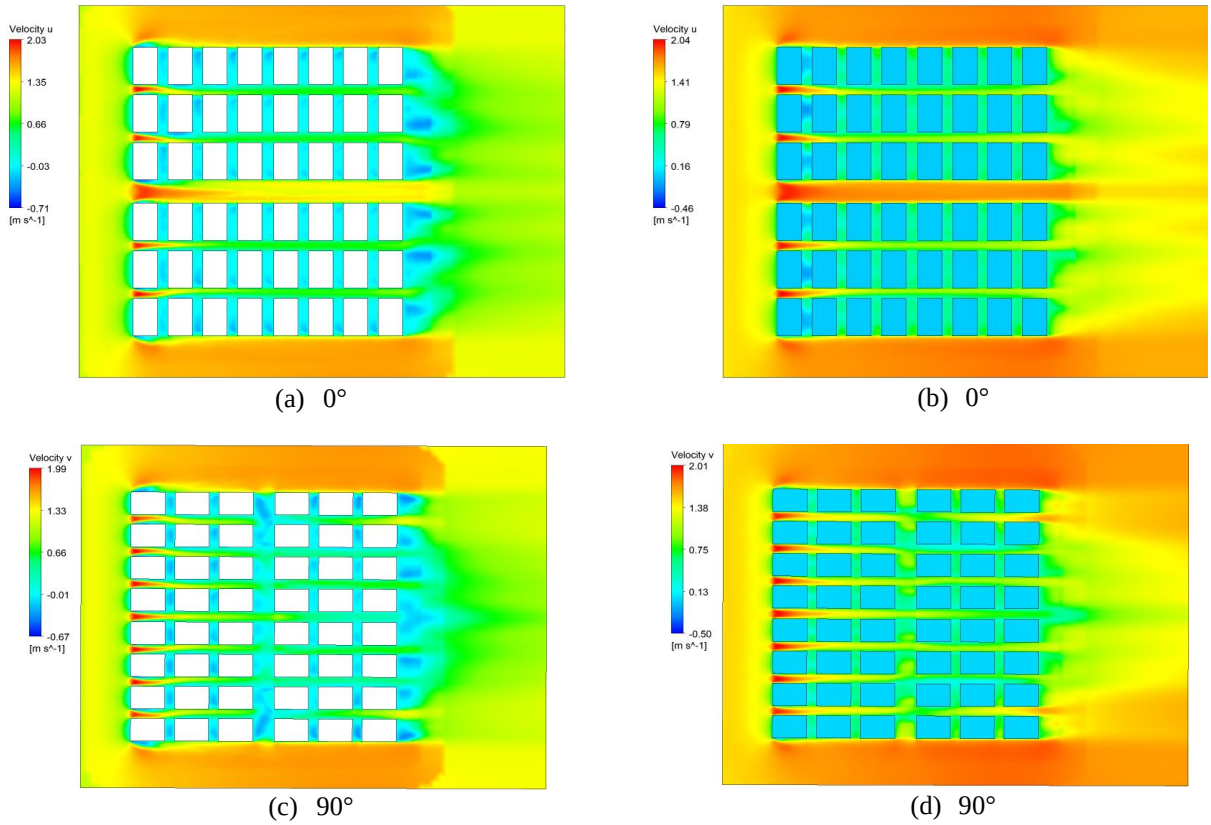

(a) 0° (b) 0°

(c) 90° (d) 90°

Figure 5. Plan view of mean horizontal velocity contours at (a) and (c) $z/H_b = 0{,}5$; (b) and (d) $z/H_b = 1$.

Figure 5(a) and (c) show mean horizontal velocity, at principal direction, inside the canopy. For both configuration, 0° and 90°, the pattern of velocity is characterized by low velocity regions and recirculation zones behind the buildings. However, for 0° wind direction, flow on the main street plays an important role on the dispersion. Note that the flow has a preferential path in the major street and could influence the dispersion of pollutants in this region. Similar behavior is observed in Figure 5(b) and (d), but instead with higher velocity magnitudes in the main street.

Figure 6 shows the streamlines of the mean velocity for different values of height above the ground. It is now possible to see the eddies (recirculation zones) that were not visible in the contour plots of Figure 5.

Figure 6(a) and (b) show the 0º wind direction case at half and at exactly the building height, respectively. Figure 4(a) exhibit the convergence and divergence of the flow field between streets together with the eddies between consecutive buildings and at the wake. In Figure 4(b) the flow field is less influenced by the buildings since most streamlines only slightly change its directions.

Figure 6(c) and (d) show the 90º wind direction case at the same heights aforementioned. In the same way, Figure 6(c) shows formation of eddies between consecutive buildings, but in this case, the major street is now perpendicular to the wind direction which results in streamlines being redirected from one street to another, which could contribute to pollutant transport from one street to another.

It is interesting to note that regions between buildings in Figure 6(a) mostly contains three eddies inside them while Figure 6(c) mostly contains only two, which can be explained by the building dimension perpendicular to the flow direction, that is larger in the first one, 350 mm, than the second one, 230 mm.

All wind direction cases presented a small region with high velocity values of about 2 ms^{-1} right at the entrance of each canopy street. This is explained by the fact that the wind is constrained by the street's width such that the pressure energy of the fluid is converted to kinetic energy at these points, yet this energy is then converted along the street to turbulent kinetic energy due to the buildings wall effect, which generates the eddies and reduces the wind speed.

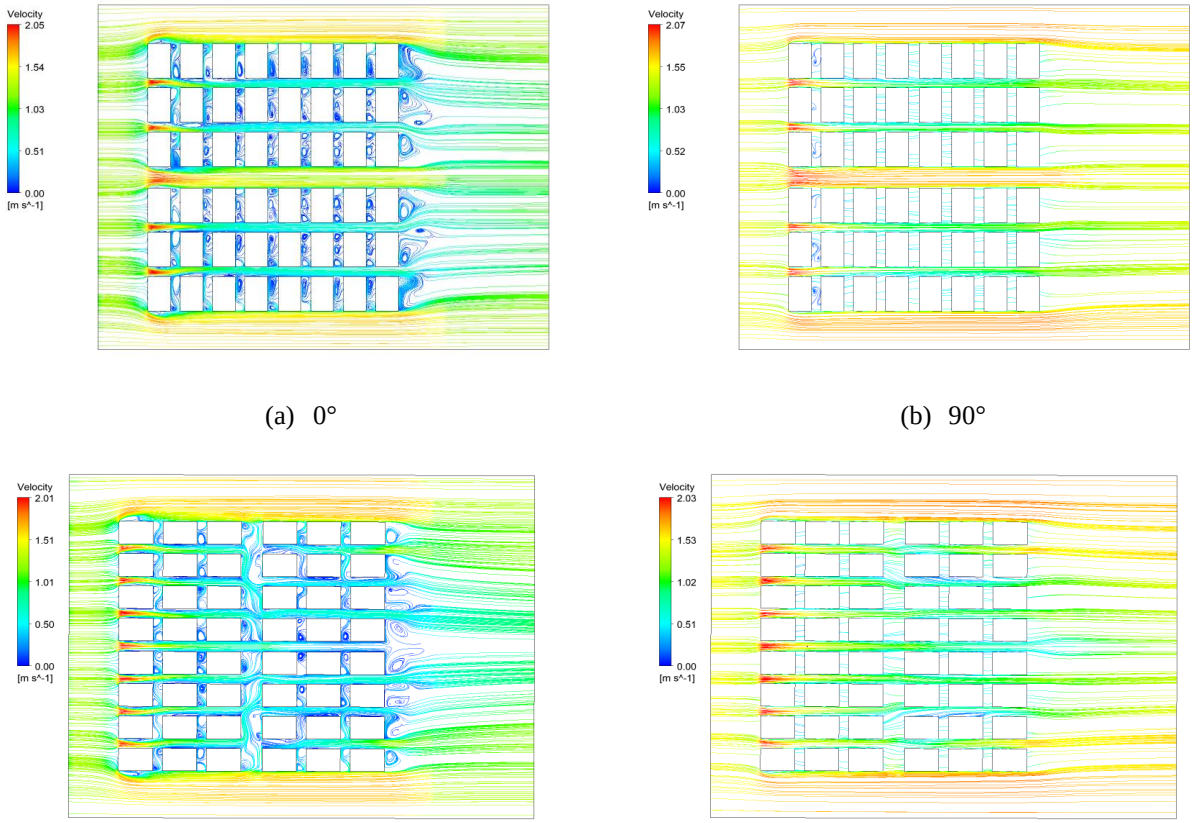

(a) 0° (b) 90°

(c) 0° (d) 90°

Figure 6. Plan view of the flow field streamlines at (a) and (c) $z/H_b = 0{,}5$; (b) and (d) $z/H_b = 1$.

4. CONCLUSIONS

This study displayed the performance of four different RANS turbulence closure models, which represented well the flow in an urban canopy of buildings with constant height when compared to available experimental data, beyond that, it was already expected that a Reynolds Stress Model would describe the flow more precisely, since these models use a transport equation for each turbulent stress instead of modelling all of them. The Standard $k - \varepsilon$ model represented the flow very well even though it is less computationally demanding, therefore, it could be used for some flow cases that do not require much precision.

The influence of wind direction was very much noticeable, given that the buildings have uneven dimensions and the streets also have different widths. The presence of a wider street parallel to the wind contributes to the appearance of a flow short-circuit, potentially reducing pollutant concentration in this area, and the building's dimension contributes to the number of eddies that appear downwind, such that with more eddies, harder it is to pollutant dispersion to occur, possibly increasing its concentration in this region. When the major street was put perpendicular to the flow, it redirected the flow from one street to a parallel one, also showing a possible path that a pollutant could take if it was released and dragged by the flow.

5. ACKNOWLEDGEMENTS

The authors gratefully acknowledge funding from Espirito Santo Research Foundation (FAPES) (Grant Term 080/2019) and Federal Institute of Espirito Santo (IFES).

6. REFERENCES

An, K., and Fung J.C.H. “An improved SST k – ω model for pollutant dispersion simulations within an isothermal boundary layer”. *Journal of Wind Engineering & Industrial Aerodynamics*. 179, 369–384, 2018.

Buccolieri, R., Salizzoni, P., Soulhac, L., Garbero, V., and Di Sabatino, S. “The breathability of compact cities”. *Urban Climate*, 13, 73–93, 2015.

Carpentieri, M., and Robins, A. G. “Influence of urban morphology on air flow over building arrays”. *Journal of Wind Engineering & Industrial Aerodynamics*. 145, 61–74, 2015.

Chen, L., Hang, J., Sandberg, M., Claesson, L., Di Sabatino, and S., Wigo, H. The impacts of building height variations and building packing densities on flow adjustment and city breathability in idealized urban models. *Building and Environment*, 118, 344–361, 2017.

Fu S., Launder B. E., and Leschziner M. A. "Modeling Strongly Swirling Recirculating Jet Flow with Reynolds-Stress Transport Closures". *In Sixth Symposium on Turbulent Shear Flows*. Toulouse, France. 1987.

Gibson M. M. and Launder B. E. "Ground Effects on Pressure Fluctuations in the Atmospheric Boundary Layer". *Journal of Fluid Mechanics*. 86. 491–511. 1978.

Goulart E. V., Reis Jr., N.C., Lavora, V.F., Castro, I.P., Santos, J.M., and Xie, Z.T. Local and non-local effects of building arrangements on pollutant fluxes within the urban canopy. *Building and Environment* 147, 23-34, 2019.

Launder B. E. "Second-Moment Closure and Its Use in Modeling Turbulent Industrial Flows". *International Journal for Numerical Methods in Fluids*. 9. 963–985. 1989.

Launder B. E., Spalding D. B. “Lectures in Mathematical Models of Turbulence”. *Academic Press*, London, England. 1972.

Menter F. R. "Two-Equation Eddy-Viscosity Turbulence Models for Engineering Applications". *AIAA Journal*. 32(8). 1598–1605. 1994.

Ramponi, R., Blocken, B., de Coo, L. B., and Janssen, W. D. “CFD simulation of outdoor ventilation of generic urban configurations with different urban densities and equal and unequal street widths”. *Building and Environment*. 92, 152–166, 2015.

Ricci, A., Kalkman, I., Blocken, B., Burlando, M., Repetto, M.P. “Impact of turbulence models and roughness height in 3D steady RANS simulations of wind flow in an urban environment”. *Building and Environment*, Volume 171, 2020.

Wilcox D. C. “Turbulence Modeling for CFD”. *DCW Industries, Inc*. La Canada, California. 1998.

7. RESPONSIBILITY NOTICE

The authors are the only responsible for the printed material included in this paper.